Synthesis and Biophysical Analysis of Transmembrane Domains of a *Saccharomyces cerevisiae* G Protein-Coupled Receptor†

Haibo Xie,‡ Fa-Xiang Ding,‡ David Schreiber,‡ Gary Eng,‡ Shi-feng Liu,‡,§ Boris Arshava,‡ Enrique Arevalo,‖ Jeffrey M. Becker,⊥ and Fred Naider*,‡

Department of Chemistry and Biochemistry, The College of Staten Island and The Graduate School of The City University of New York, Staten Island, New York 10314, and Department of Biochemistry, Cellular and Molecular Biology, University of Tennessee, Knoxville, Tennessee 37996

Received June 22, 2000

ABSTRACT: The Ste2p receptor for α-factor, a tridecapeptide mating pheromone of the yeast *Saccharomyces cerevisiae*, belongs to the G protein-coupled family of receptors. In this paper we report on the synthesis of peptides corresponding to five of the seven transmembrane domains (M1−M5) and two homologues of the sixth transmembrane domain corresponding to the wild-type sequence and a mutant sequence found in a constitutively active receptor. The secondary structures of all new transmembrane peptides and previously synthesized peptides corresponding to domains 6 and 7 were assessed using a detailed CD analysis in trifluoroethanol, trifluoroethanol−water mixtures, sodium dodecyl sulfate micelles, and dimyristoyl phosphatidyl choline bilayers. Tryptophan fluorescence quenching experiments were used to assess the penetration of the membrane peptides into lipid bilayers. All peptides were predominantly (40−80%) helical in trifluoroethanol and most trifluoroethanol−water mixtures. In contrast, two of the peptides M3-35 (KKKNIIQVLLVASIETSLVFQIKVIFTGDNFKKKG) and M6-31 (KQFDSFHILLINleSAQSLLVPSIIFILAYSLK) formed stable β-sheet structures in both sodium dodecyl sulfate micelles and DMPC bilayers. Polyacrylamide gel electrophoresis showed that these two peptides formed high molecular aggregates in the presence of SDS whereas all other peptides moved as monomeric species. The peptide (KKKFDSFHILLIMSAQSLLVLSIIFILAYSLKKKS) corresponding to the sequence in the constitutive mutant was predominantly helical under a variety of conditions, whereas the homologous wild-type sequence (KKKFDSFHILLIMSAQSLLVPSIIFILAYSLKKKS) retained a tendency to form β-structures. These results demonstrate a connection between a conformational shift in secondary structure, as detected by biophysical techniques, and receptor function. The aggregation of particular transmembrane domains may also reflect a tendency for intermolecular interactions that occur in the membrane environment facilitating formation of receptor dimers or multimers.

G protein-coupled receptors (GPCRs)[1] mediate the transduction of a plethora of signals from the outside surface of a cell to its cytoplasmic interior (*1*−*3*). To date, nearly 1000 examples of this family of signal transduction proteins have been reported (*4*). Representative examples include photoreceptors, chemotactic receptors, the β-adrenergic receptors, and a variety of receptors that recognize small and medium sized polypeptides. Numerous mutagenesis studies have been carried out on GPCRs, and reports on ligand−receptor contact points are appearing with increasing frequency. In several cases detailed models for the ligand−receptor complex have been reported (*5*, *6*).

Despite the successes achieved in understanding the mechanism of action of GPCRs, only modest experimental support exists for their three-dimensional structures. Detailed information on the 3D structure of an integral membrane protein derives from X-ray and electron microscopy analysis on bacteriorhodopsin. This photoreceptor protein has been crystallized, and its structure is available at a resolution of 3 Å (*7*−*9*). The analysis indicates that the protein has seven transmembrane domains, which are primarily α-helical and which are arranged in a compact, roughly elliptical structure when viewed from above the plane of the membrane. On the basis of a detailed analysis of sequence data of various

† This work was supported by research grants GM22086 and GM22087 from the National Institute of Health and by a grant from the PSC−CUNY Research Award Program. F.N. is currently Varon Visiting Professor at the Weizmann Institute of Science Rehovot.

* Correspondence should be addressed to this author. Telephone: (718) 982-3896. Fax: (718) 982-3910. E-mail: naider@postbox.csi.cuny.edu.

‡ Department of Chemistry, The College of Staten Island and the Graduate School of The City University of New York.

§ Current address: Department of Chemistry, University of Waterloo, Ketchener, Ontario N2M 5G4, Canada.

‖ Department of Biochemistry, The Graduate School of The City University of New York.

⊥ University of Tennessee.

[1] Abbreviations: ATR-FTIR, attenuated total reflectance Fourier transform infrared; CD, circular dichroism; DMPC, 1,2-dimyristoyl-*sn*-glycero-3-phosphocholine; DMPG, 1,2-dimyristoyl-*sn*-glycero-3-[phospho-*rac*-(1-glycerol)]; EDT, 1,2-ethanedithiol; GPCRs, G protein-coupled receptors; HBTU, *O*-benzotriazolyl-*N*,*N*,*N*′,*N*′-tetramethyluronium hexafluorophosphate; HPLC, high-performance liquid chromatography; MES, 2-(*N*-morpholino)ethanesulfonic acid; SDS, sodium dodecyl sulfate; SDS-PAGE, SDS polyacrylamide gel electrophoresis; TFA, trifluoroacetic acid; TFE, 2,2,2-trifluoroethanol; TM, transmembrane; UV, ultraviolet.

10.1021/bi001432p CCC: $19.00
Published on Web 11/16/2000

G protein-coupled receptors, the arrangement of the seven transmembrane helices has been predicted to be counterclockwise beginning from helix 1 near the amino terminus and proceeding to the carboxyl terminus (*10).* Very recently, the structure of the GPCRs rhodopsin was solved at 2.8 Å resolution (*11*). Despite the elegant studies on bacteriorhodopsin and its G protein-coupled homologue, rhodopsin, very little information is available on the structure of other GPCRs. The pathway of folding of these molecules is also relatively virgin territory. Although various hydropathy algorithms are useful in placing putative transmembrane domains within the primary sequence of these receptors, direct evidence for either the authenticity of these placements or the stability of the domains is lacking.

A two-step folding mechanism has been developed for integral membrane proteins in which the α-helices first insert into the phospholipid bilayer and then, in a second step, associate into the final three-dimensional structure of the biomolecule (*12*). This model infers spontaneous folding of the integral membrane protein and suggests that both intact receptors and fragments of receptors would refold to biologically active species. In vitro evidence supporting this hypothesis has been presented for bacteriorhodopsin (*13*, *14*) and for fragments of this protein (*15*−*17*). In addition, coexpressed polypeptide fragments of rhodopsin were demonstrated to spontaneously assemble into functional receptor in COS-1 cells (*18*).

Experience with individual transmembrane domains suggests that they are highly insoluble and have marked tendencies to form intractable aggregates. Since short fragments of receptors are amenable to biophysical analysis using nuclear magnetic resonance techniques, information concerning their structural tendencies and the relevance of these tendencies to the structure and function of the cognate integral membrane protein is highly desirable. An early report provided circular dichroism (CD) evidence that two transmembrane domains of the α-factor receptor of *Saccharomyces cerevisiae* formed stable helices in trifluoroethanol (TFE) and trifluoroethanol−water mixtures (*19*). Recently, the detailed structure of one of these helices was determined by NMR to contain a kink at a Pro residue predicted to be in the middle of the membrane (*20*). An extensive study on peptides representing the seven transmembrane helices of bacteriorhodopsin presented CD, IR, and proton deuterium exchange data which indicated that the peptides corresponding to helices A−H of this protein had very different biophysical tendencies and structural stabilities (*21*). NMR studies on several cytoplasmic loops and the carboxyl terminus of rhodopsin suggested that these receptor domains were stabilized by short-range interactions and assumed secondary structures such as *β*-turns and α-helices (*22*−*24*). Very recently, a high-resolution structure of a 15-residue portion of the sixth transmembrane domain of rhodopsin was reported (*25*).

It is valid to inquire as to the biological relevance of studies on relatively short peptides conforming to regions of large integral membrane proteins. One might argue that despite the individual conformational tendencies of these peptides, the structures of all regions of the receptor are influenced by long-range interactions between various domains. However, as indicated by the above studies on rhodopsin and bacteriorhodopsin, it is clear that regions of receptors maintain functional relevance. Specifically, in the case of rhodopsin, three fragments representing transmembrane helices 1−3, 4−5, and 6−7 re-formed a functional pigment in the membrane of COS-1 cells (*18*). Recently, a similar analysis was made on the G protein-coupled receptor (Ste2p) for the mating factor of yeast. Coexpressed fragments representing splits in every loop of the receptor re-formed a protein which signaled in response to the peptide pheromone (*26*). This study supports the notion that biophysical analysis of receptor fragments should provide structural information that is relevant to the assembly and stability of the intact Ste2p. The general features of the topology of this GPCR have been verified using gene fusion and protein reporter methodologies (*27*, *28*). In this paper we report on the synthesis of five of the seven transmembrane domains and two homologues of the sixth transmembrane domain (Figure 1 illustrates a cartoon representation of Ste2p), on a detailed CD analysis of the seven transmembrane domains in trifluoroethanol, trifluoroethanol−water mixtures, sodium dodecyl sulfate micelles, and dimyristoyl phosphatidyl choline bilayers, and on the properties of these receptor domains in polyacrylamide gels. Tryptophan fluorescence and quenching experiments were used to assess the penetration of the membrane peptides into lipid bilayers. The analysis reveals very different biophysical properties for these peptides and provides new insights into domain−domain interactions that might occur in the intact receptor.

EXPERIMENTAL PROCEDURES

Materials

Wang resin and Fmoc-protected amino acids were purchased from Advanced ChemTech (Louisville, KY) except Fmoc-His(Trt), which was purchased from Calbiochem-Novabiochem Corp. (San Diego, CA) and Bachem Inc. (Torrance, CA). Diisopropyl-ethylamine (DIEA), dicyclohexylcarbodiimide (DCC), trifluoroacetic acid (TFA), thioanisole, 1,2-ethanedithiol (EDT), *N*,*N*′-dimethyl-aminopyridine (DMAP), 2-(*N*-morpholino)ethanesulfonic acid (MES), sodium dodecyl sulfate (SDS), and all other reagents were purchased from Aldrich Chemical Co. (Milwaukee, WI). Solvents used for synthesis and purification were purchased from VWR Scientific (Piscataway, NJ) and Fisher Scientific (Springfield, NJ). Dimyristoylphosphocholine (DMPC) and dimyristoylphosphglycerol sodium salt (DMPG) were purchased from Avanti Polar Lipid (Alabaster, AL).

Peptide Design and Synthesis

The peptides synthesized in this report are predicted by hydropathy analysis to be the first through the fifth of seven transmembrane domains (see Table 1 for list of peptides studied): M1-33 (44−77, C59A) [in this abbreviation for the peptide studied, M1 represents the first transmembrane domain predicted for Ste2p, see Figure 1, 33 denotes the number of residues in the synthetic polypeptide, 44−77 are the residues of Ste2p contained in the peptide with residue 1 being the N-terminal residue of Ste2p, and C59A denotes a substitution of Ala in the synthetic peptide for Cys of the native Ste2p], M2-35 (74−108), M3-35 (132−160 plus six additional residues), M4-36 (163−190 plus eight additional residues), M5-38 (198−235, M218Nle), and two homologues

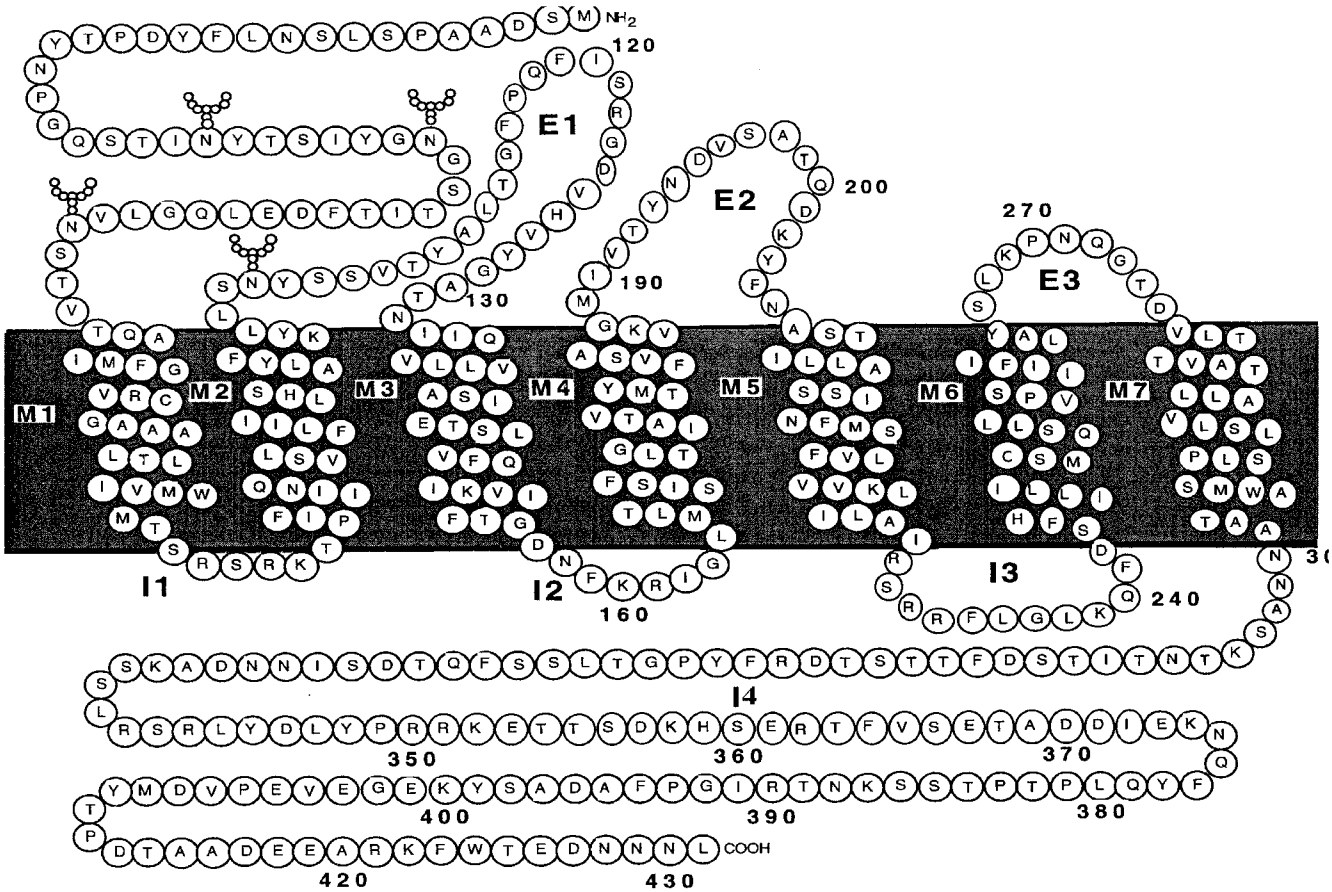

FIGURE 1: Cartoon of the α-factor receptor (Ste2p). Domains are indicated by the following: E, extracellular loops; I, intracellular loops; M, transmembrane domains. Four of the Asn residues are represented as glycosylation positions.

Table 1: Sequences and Names of Transmembrane Peptides of Ste2p

name[a]	residue[b]	Φ[c]	sequence[d]
M1-33	45−77, C59A[e]	1.82 (52−71)	VNSTVTQAIMFGVR**A**GAAALTLIVMWMTSRSRK
M2-35	74−108	1.95 (80−99)	RSRKTPIFIINQVSLFLIILHSALYFKYLLSNYSS
M3-35	132−160	1.66 (135−154)	**KKK**NIIQVLLVASIETSLVFQIKVIFTGDNFK**KKG**
M4-36	163−190	1.46 (166−185)	**KKK**GLMLTSISFTLGIATVTMYFVSAVKGMI**KKKKG**
M5-38	198−235, M218Nle[e]	2.23 (209−228)	ATQDKYFNASTILLASSINF**Nle**SFVLVVKLILAIRSRRF
M6-35L	241−269, C252A, P258L[e]		**KKK**FDSFHILLIMS**A**QSLLV**L**SIIFILAYSLK**KKS**
M6-35P	241−269, C252A[e]		**KKK**FDSFHILLIMS**A**QSLLV**P**SIIFILAYSLK**KKS**
M6-31[f]	239−269, M250Nle,[e] C252Ae	2.36 (246−265)	KQFDSFHILLI**Nle**S**A**QSLLVPSIIFILAYSLK
M7-30[f]	273−302	1.47 (278−297)	GTDVLTTVATLLAVLSLPLSSMWATAANNA

[a] M = transmembrane domain; the first number follows the order of the transmembrane domains in the receptor, the second number represents the total number of residues in the peptide. [b] The numbering system used in this report assigns the amine terminal residue (Met1) as position 1 and the carboxyl terminal residue (Leu431) as residue 431. [c] Average hydrophobicities were calculated for 20 residues of each receptor domain predicted to be in the membrane (Figure 1) *(29)*. Numbers in the parentheses represent the first and the last residues for each domain. [d] The bold and underlined amino acids represent additional residues or mutant residues. [e] The letters in front of the number represent original residues and those behind mutant ones. [f] Previously synthesized compounds (*19*, *20*).

of the sixth transmembrane domain, M6-35P (241−269, C252A, a total of five artificial Lys residues were added to the termini of this peptide, Table 1), and M6-35L (241−269, C252A, P258L, a total of five artificial Lys residues were added to the termini of this peptide, Table 1). The syntheses of M6-31 (239−269, M250Mle C252A) and M7-30 (273−302) were reported previously (*19*, *20*). The amino acid sequences of the new peptides are indicated explicitly in Table 1. On the basis of our previous experience with peptides M6-31 and M7-30, the charge density of the transmembrane sequences is a crucial factor in determining the overall solubility properties of these highly hydrophobic polypeptides. To improve solubility, peptides were designed to include four or five residues which were predicted to reside in the interhelix loops on both sides of a given helix (Table 1). However, using the wild-type sequences, the solubility of the M3 and M4 domains was very low and severe precipitation was encountered during HPLC purification attempts. To circumvent this difficulty, several additional lysines with positive-charged side chains were added to both termini (Table 1) to increase solubility and decrease the aggregation of peptide chains. This approach has also been used by other investigators (*30*, *31*). The syntheses of these latter peptides were carried out starting with the Fmoc-Gly-Wang resin because it was available with low loading. In the case of M1-33 and M5-38, Cys[59] and Met[218] were

replaced with Ala and Nle, respectively, to eliminate synthetic problems from oxidation of Cys and Met. Similar replacements had been employed in previous studies on M6-31 and M7-30 (*19*, *20*). Moreover, mutated receptors containing similar replacements retained signaling activity (*26*; Arevalo, unpublished results).

All peptides were synthesized in a stepwise manner on a 0.1 mmol scale using an Applied Biosystems Inc. Model 433A synthesizer. The coupling strategy utilized FastMoc chemistry with the use of extended coupling times. Double-coupling was carried out for each residue using HBTU/HOBt activation, and capping was accomplished with acetic anhydride in the presence of DIEA. The Fmoc group was used for protection of all N-α groups, and Boc, Trt, Trt, tBu, tBu, tBu, and Pmc were employed for protection of Lys, Gln, His, Ser, Tyr, Asp, and Arg, respectively. All Fmoc groups were removed in 20% piperidine in NMP. After the completion of chain assembly, the N-terminal Fmoc group was removed and the resin was treated with a solution of either 0.75 g of phenol, 0.5 mL of thioanisole, 0.25 mL of EDT, 0.5 mL of water, and 10 mL of TFA if the peptide contained Arg or Met or of 9.5 mL of TFA, 0.25 mL of EDT, and 0.25 mL of water if the peptide contained neither Arg nor Met but contained Trt or Trp. The reaction was carried out at room temperature for 1−2 h, the reaction mixture was filtered, and the filtrate was concentrated to a small volume on a rotatory evaporator. The crude peptides were precipitated by addition of anhydrous ether.

Peptide Purification

Analytical reversed phase HPLC (RP-HPLC) was performed using a Vydac column (259VHP54 polymer column; 4.6 mm × 250 mm) at 80 °C and elution with water−acetonitrile or water−methanol (all containing 0.1% TFA) linear gradients. In the case of M3-35, only a water−methanol (both containing 0.1% TFA) linear gradient achieved resolution of the crude peptide. Semipreparative HPLC was run on a Vydac 259VHP510 polymer column (10 mm × 250 mm) with a water jacket at 55−65 °C. Detection was at 220 nm. All peptides were purified to over 98% homogeneity as judged by RP-HPLC. The final products were assessed by electrospray mass spectrometry (ES-MS) and amino acid analysis. ES-MS was performed at Peptido Genic Research & Company, Livermore, CA. Amino acid analyses were performed at the Biopolymer Laboratory Brigham and the Women's Hospital of Harvard Medical School after acid hydrolysis with 6 N HCl for 72 h at 110 °C.

Buffers

The MES buffer contained 10 mM 2-(*N*-morpholino)-ethanesulfonic acid (MES), adjusted to pH 6.4 with KOH. The SDS buffer contained 0.5% SDS (w/v), 30 mM $NaHPO_4$, and 0.025% NaN_3, pH 7.9−8.0. For experiments where SDS was used at pH 6.0, the pH was adjusted by addition of 1 M HCl. Buffers used in the SDS-PAGE studies are as reported by Schagger and von Jagow (*32*).

Circular Dichroism Spectroscopy

(1) Sample Preparation in SDS or DMPC Vesicles. (A) In SDS Buffer. The purified lyophilized peptide was dissolved at 2 mg/mL in TFE; this solution was diluted with 9 vol of 0.5% SDS (w/v) prior to the initiation of dialysis against buffer. Dialysis was performed in Spectrapor 6 dialysis tubing (MWCO 1000). The volume of the dialysis buffer was at least 200−300 times that of the hydro-organic mixture, and the buffer was changed twice during a total period of 48−72 h dialysis. The buffer had a pH of 8.0 for the initial round of dialysis and a pH of 6.0 for the subsequent two rounds.

(B) In DMPC Vesicles. To 100 μL of stock peptide solution (2 mg/mL TFE) was added 300 μL of 1.2 mg of DMPC in chloroform. The solvent was removed by rotary evaporation under a stream of nitrogen, and the remaining peptide−lipid residue was placed in a vacuum desiccator for several hours to eliminate the last traces of solvent. Buffer (0.5 mL of MES) was added to the peptide−lipid mixture, and hydration was accomplished by vortexing for 1 min and sonication at 30 °C with a Misonix Inc. W-385 sonicator equipped with a cup horn until homogeneity and transparency were obtained. In the case of M1-33, a modified procedure was used because the above procedure failed to result in a clear solution: 100 μL of M1-33 stock solution (2 mg/mL TFE) was treated as above. After hydration in MES buffer and vortexing for 1 min, 50 μL of TFE was added and the resultant solution was sonicated at 30 °C until homogeneity and transparency were obtained. This solution was then dialyzed with MES buffer for 3 days. The volume of the dialysis buffer was at least 200−300 times that of the mixture, and the buffer was changed twice. This method resulted in a transparent solution of M1-33 in DMPC bilayers.

(2) Spectroscopic Measurements. The CD spectra of the peptides were recorded on an AVIV model 62 DS CD instrument (AVIV associates, Lakewood, NJ), which was interfaced with a computer used for all mathematical calculations. A 1 mm sample cell with a thermostated cell holder was used for all spectral studies: bandwidth, 1 nm; averaging time, 0.5 s; repeated 6 times. Peptide concentrations in solution were determined from amino acid analysis. Prior to calculation of the final ellipticity, all spectra were corrected by subtracting the reference spectrum. CD intensities are expressed as mean residue ellipticities (deg·cm^2/dmol).

(3) Estimation of Percent α-Helicity. Estimation of percent α-helicity was made using a method initially suggested by Greenfield and Fasman (*33*) and later modified by Wu et al. (*34*) and Chen et al. (*35*). These methods use ellipticities at either 208 or 222 nm and calculate fractional helicities as follows:

$$f_h = ([\theta]_{222} - [\theta]^0_{222})/([\theta]^{100}_{222} - [\theta]^0_{222})$$

where $[\theta]_{222}$ is the experimentally observed mean residue ellipticity at 222 nm and values for $[\theta]^0_{222}$ and $[\theta]^{100}_{222}$, corresponding to 0 and 100% helical content at 222 nm, were estimated to be 2000 and 30 000 deg·cm^2/dmol, respectively (*34*, *35*). When the wavelength used is 208 nm, the 0% and 100% helicities were 4000 and 33 000 deg·cm^2/dmol, respectively (*33*).

Fourier Transform Infrared Spectroscopy (FTIR)

(1) Preparation of Lipid-Peptide Vesicles for FTIR. Transmembrane domain peptide M6-35L or M6-35P (0.27

mg in 0.27 mL of TFE) was added to 4 mg of DMPC/DMPG (4:1) in $CHCl_3$/MeOH (1:1). The resulting solution was dried under N_2 flow. Residual traces of organic solvent were removed by placing the dried film under vacuum overnight, and the lipid was suspended in 1 mL of 0.1 mM phosphate buffer, pH 6.3. The suspension was sonicated at approximately 50 °C for 30 min in a Misonix Inc. W-385 sonicator equipped with a cup horn (40% output power). The vesicle solution was further exhausted dialyzed into 600 mL of 0.1 mM phosphate buffer, pH 6.3. The resulting vesicles were then passed through a 0.45 μm polycarbonate centrifugal filter. The calculated molar ratio of peptides to lipid was 1:108.

(2) FTIR Spectroscopy. FTIR spectra were recorded at ambient temperature (~20 °C) on a Nicolet Magna 550 Fourier transform infrared spectrometer (Nicolet Analytical Instruments, Madison, WI) equipped with a DTGS detector. For each sample, 1000 interferograms recorded at a spectral resolution of 4 cm^{-1} were averaged and processed using 1.0 filling and Happ−Genzel apodization. A total of 100 μL of the preformed lipid vesicles with or without peptide were dried on the surface of CaF_2 window (25 mm diameter and 4 mm depth).

Fluorescence Quenching of TM1-33 in Vesicle or Methanol by KI

(1) Preparation of Lipid−Peptide Vesicles. To 100 μL of M1-33 or M7-30 solution (1 mg/mL TFE) was added a solution of 1 mg of dimyristoyl phosphocholine (DMPC) in 0.5 mL of chloroform. The resulting solution was dried under a stream of N_2. Residual traces of organic solvent were removed by placing the dried film under vacuum overnight, and the lipid was hydrated in 10 mL of MES buffer (10 mM, pH 6.3). The suspension was sonicated at approximately 50 °C for 60 min with a Misonix Inc. W-385 sonicator equipped with a cup horn. The resulting vesicles were then passed through a 0.45 μM polycarbonate centrifugal filter. The molar ratio of peptide to lipid was 1:500. Since the concentration in the fluorescence experiments was much lower than that used in the CD work, filtration of the sample worked. However, at the CD concentrations, filtration resulted in loss of peptide.

(2) Fluorescence Spectroscopy. Fluorescence measurements were recorded using a Spex Fluoromax fluorometer (Instrument S. A. Inc., Edison, NJ) with a 1 cm × 1 cm quartz cuvette. A total of 2 mL of sample was stirred continuously with a magnetic bar. The emission spectra were scanned between 300 and 420 nm with an excitation wavelength of 280 nm at intervals of 1 nm with a 1 s integration time at each wavelength. Both the excitation and emission bandwidths were 3 nm. The fluorescent intensities, calculated by integration within the emission range, minus the intensities of control alone (vesicles or methanol) at appropriate KI and KCl concentrations were used to calculate the quenching constants. The presented data were averaged from three independent measurements.

(3) Collisional Quenching Experiments. Lipid−peptide vesicle solution was stirred in a cuvette for half an hour. Fluorescence collisional quenching experiments with iodide were performed by sequentially adding a 4 M KI solution in 10 mM MES buffer to a final KI concentration of 56 mM. After addition of the peptide, the solution was allowed to equilibrate for 5−10 min and the fluorescence was measured. Changes in fluorescence due to the addition of quencher were corrected by subtracting the fluorescence measured in DMPC vesicle control. The quenching constant (K_{sv}) of the fluorescence emission at the maximum wavelength (342 nm) was determined from the slope of a plot of F_0/F vs iodide concentration [I^-] as per the Stern−Volmer equation:

$$F_0/F = 1 + K_{sv}[I^-] \quad (1)$$

where F_0/F is the ratio of fluorescence intensities in the presence of KCl and KI.

Tricine−SDS-PAGE Studies on Transmembrane Peptides

The purity and oligomeric state of synthetic transmembrane peptides dissolved in SDS were investigated by gel electrophoresis. The buffer system of Schagger and von Jagon **(***32***)** was employed. Briefly, peptides dissolved in 0.5% (17 mM) SDS and 3 mM phosphate buffer (pH 6.0) were diluted 1-fold with 1 × SDS loading buffer containing the tracking dye Serva Blue G. Samples were heated at 50 °C for 3 min and centrifuged and then loaded onto a 27.7% polyacrylamide−Tricine−SDS gel and separated at a constant 120 V. After gel electrophoresis, the gel was placed in BIO-RAD fixative enhancer solution (containing 50% methanol, 10% acetic acid, 10% fixative enhancer concentrate, and 30% distilled water) and the gels were fixed with gentle agitation for 20 min. Peptides were visualized by staining with either Commassie blue or silver stain reagent.

RESULTS

Synthesis and Purification of the TMDs

All TM peptides examined in this study were prepared using solid-phase peptide chemistry. The convention used to name peptides in this article is included in Table 1. New peptides were synthesized on a Wang resin using α-Fmoc protection strategies and HBTU/HOBT activation. Membrane peptides usually contain regions which are predominantly hydrophobic, and peptide chains which are assembled on the resin matrix can form aggregates either with other peptide chains or with the polymer support. The formation of β-sheet structures may also result in incomplete solvation and poor penetration of the coupling reagents through the resin beads (*36*). Moreover, difficulty is encountered during analytical and preparative HPLC of membrane peptides due to their insolubility in the mobile phases, tendency to precipitate, and irreversible adsorption to the column material. It was found that each transmembrane domain peptide behaved differently making it difficult to develop a universal approach during purification. Thus, different procedures were applied to each individual peptide using some of the approaches described below. In general, the syntheses of M1-33, M2-35, and M5-38 were less problematic than those of M3-35 and M4-36. After cleavage from the resin, these latter were almost insoluble, and several additional flanking lysines had to be added to both termini to attain dissolution in solvents which were suitable for HPLC purification. In general, the order of synthetic difficulty with the transmembrane domains of Ste2p was M3-35/M4-36 > M1-33/M5-38 ≫ M2-35.

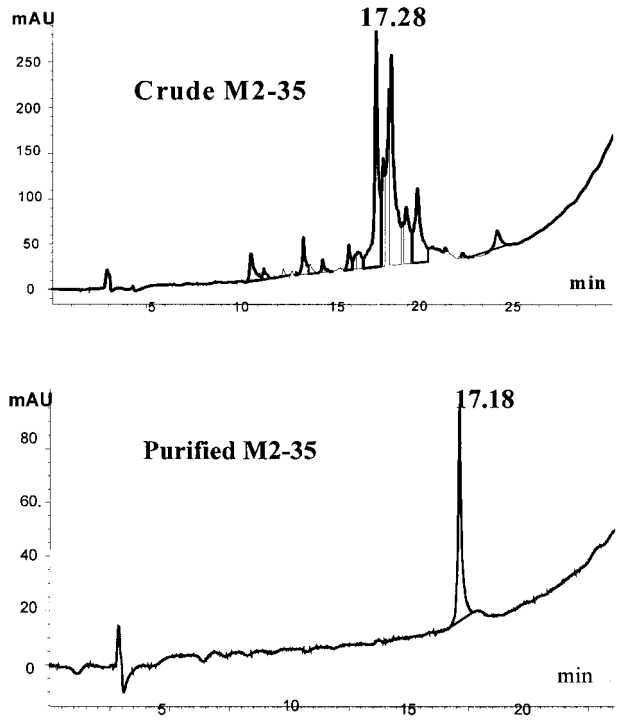

FIGURE 2: HPLC spectra of synthetic membrane peptides. Data from M2-35 is presented as a representative example. The chromatography was performed on a Vydac 259VHP54 polymer column (4.6 mm × 250 mm) at 80 °C: gradient, 90−0% A in 30 min; A, water (0.1% TFA); B, acetonitrile (0.1% TFA), $\lambda = 220$ nm.

For peptide purification, we noted that traditional RP-HPLC using a C_{18} or C_4 column did not result in either high-purity product or acceptable recoveries after HPLC for most of these transmembrane peptides. A column containing a highly cross-linked polystyrene−divinylbenzene polymer in the form of rigid, porous (300 Å pore diameter) spheres (Vydac polymer 259VHP RP column) was found to be useful in these studies. The 259VHP polymer matrix is chemically resistant to acid and alkali from pH 0 to 14, is heat stable up to 80 °C, and can be operated at a pressure up to 3000 psi. Using this column, the M1−M5 transmembrane domains were purified to >98% homogeneity as evidenced by analytical RP-HPLC (data not shown). Figure 2 illustrates the HPLC spectra of crude and purified M2-35 as a representative example. The purified peptides gave molecular weights within 2 Da of calculated values as judged by electrospray mass spectrometry (data not shown). The amino acid ratios were also consistent with the composition of the transmembrane peptides except for low Ser and Thr values, which we have observed before and believe are due to degradation of the residues during the extended hydrolysis reaction (*20*). The presence of intact Trp in M1-33 and M7-30 was verified by absorption measurements and fluorescence spectroscopy.

During purification of the membrane peptides it was observed that recoveries using the polymer-based column were dependent on a variety of factors such as temperature, elution solvents, flow rate, and gradient. Increasing the column temperature during analytical HPLC resulted in significant changes in peak intensity, suggesting that aggregation may decrease at elevated temperatures resulting in improved resolution (data not shown). Accordingly, HPLC was carried out above room temperature, usually at 80 °C for analysis and 65 °C for purification. Further improvement was also observed with M3-35 when a methanol−water gradient was used (data not shown). It is clear that the successful isolation of membrane peptides will benefit from investigations with a variety of mobile phases at different temperatures. Conclusions based on one mobile system can be highly misleading with respect to the quality of the synthesis achieved (*31*).

Table 2: Calculated Helicities (%) for M1−M7 in Different Membrane Mimetic Environments[a]

	TFE/water				0.5%	3.6 mM
peptide	100%	75%	50%	25%	SDS	DMPC
M1-33	68	65	60	50	73	63
M2-35	79	72	67	60	50	43
M3-35	72	73	77	64	*b*	*b*
M4-36	86	85	80	75	79	72
M5-38	68	62	60	56	47	42
M6-31	57	43	44	27	*b*	*b*
M7-30	75	58	54	45	36	38

[a] Calculated using $[\theta]_{222}$ values (see Experimental Procedures). [b] Not calculated due to low α-helicity.

CD Analysis

The shape and intensity of the CD spectrum between 180 and 240 nm are sensitive to protein secondary structure. As the Ste2p receptor protein is localized to the plasma membrane in *Saccharomyces cerevisiae*, the seven TM peptides were analyzed by CD in membrane mimetic solvents including aqueous TFE, SDS buffer, and DMPC vesicles. Quantitative analysis of these CD spectra were carried out using the ellipticity at 222 nm to approximate percent α-helicities as described in Experimental Procedures. Similar calculations based on the ellipticity at 208 nm were also carried out and gave almost identical results (data not shown). Although more sophisticated algorithms for deconvoluting CD spectra are available, most of these have been optimized for proteins. Attempts to apply several algorithms such as Contin and PROSEC to deconvolute the CD spectra of the transmembrane peptides failed to give meaningful results in that negative percentages were calculated for certain secondary structures. Others have noted difficulty in the application of these algorithms to membrane peptides (*21*). We believe that $[\theta]_{222}$ approximation is sufficient for the comparative purpose of this study, and the results on the seven transmembrane domains of Ste2p are summarized in Table 2. It should be noted that calculations that are based on the mean residue ellipticity at 222 nm are not significantly affected by the presence of His residue (e.g., in M2-35), since the contribution of the imidazole chromophores to the CD spectrum at 222 nm is negligible (*37*, *38*).

The CD spectra of the seven transmembrane peptides in TFE−water from 100% TFE to 50% TFE are all characterized by double minima at 222 and 208 nm and a ratio of the magnitude of the molar ellipticity at 195 nm vs at 222 nm greater than or equal to 2:1 (Figure 3). These characteristics are expected for peptide chains in primarily α-helical conformations (*39*). Despite the similarities, the different transmembrane peptides in TFE show individual responses to water titration. For example, M4-36 remains highly helical even in 25% TFE/75% water whereas the helicity of M6-31

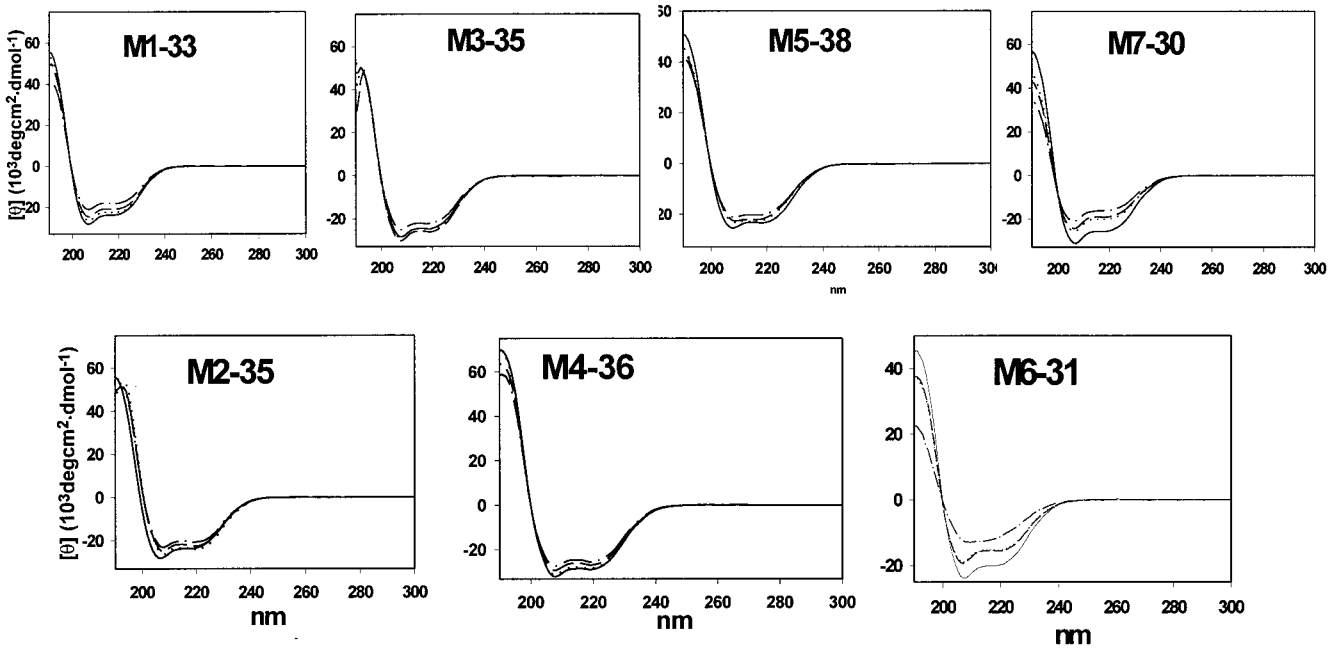

FIGURE 3: CD spectra of synthetic membrane peptides in TFE−water. Samples were dissolved in TFE and incubated at 50−60 °C for several hours. The resultant stock solutions were then diluted with TFE and/or water. In each panel, the solid line represents peptide in 100% TFE; dotted line, 75% TFE; dashed line, 50% TFE; and dots and dashes, 25% TFE. The final peptide concentrations ranged from 20 to 70 μM.

falls to 27% and the shape of the CD curve changes significantly under these conditions (Figure 3, Table 2). As summarized in Table 2, the helicity was calculated to be 40% or greater for all the peptides in 50% TFE−water with a range between 44% and 85%. As expected, none of the peptides were soluble in 100% water and CD analysis could not be undertaken in this solvent.

CD spectra of four M2 fragments with increasing chain length, M2-16 (93−108), M2-20 (89−108), M2-25 (84−108), and M2-35 (74−108; RSRKTPIFIINQVSLFLIILHSALYFKYLLSNYSS, where the R at the N terminus is 74 and the S at the C terminus is 108), were run to study the effect of chain length on the secondary structure of membrane peptides in TFE−water mixtures (data not shown). Under all conditions, every peptide was at least partially helical. Quantitative analysis on the spectra indicated that M2-25 was the most helical in all solvent mixtures, whereas M2-16 had the lowest percent helicity. M2-35 and M2-20 had similar helicities (data not shown).

The secondary structures of the transmembrane domains were also examined in media which contained micelles and lipid bilayers. In the detergent SDS, M1-33, M2-35, M4-36, M5-38, and M7-30 were helical as judged by the split $\pi-\pi^*$ transition and the significant $n-\pi^*$ transition at 222 nm (Figure 4). Similar results were obtained for these peptides in DMPC bilayers (Figure 4). Helicity was calculated to vary from ~35% to ~80% (Table 2). In contrast to spectra for these peptides, CD patterns for M3-35 and M6-31 in both SDS and DMPC exhibited a broad minimum centered near 215 nm and a maximum near 200 nm (Figure 4). These patterns are similar to standard spectra for peptides in a β-conformation. To investigate whether the β-structures would revert to helices, we carried out CD measurements of M6-31 at different concentrations. Figure 5 shows that lowering concentration from 150 to 18 μM did not result in significant changes in ellipticity (<1%) or peak position. The major variation was observed upon dilution from 18 to 6 μM with the mean residue ellipticity at 214 nm changing by 30%. Nevertheless, even at 6 μM, the CD pattern for M6-31 was totally different from that of a helical peptide. As in TFE−water mixtures, the chain length dependence for helix formation in both SDS and DMPC environments revealed that M2-25 was the most helical followed by M2-20 $\approx$ M2-35 > M2-16 (data not shown).

The thermal stability of these membrane peptides in SDS micelles was examined by raising the temperature in steps, allowing equilibrium to be obtained, and then measuring the CD spectrum (see Experimental Procedures). The helicity of M4-36 decreased gradually as the temperature was raised to 85 °C (Figure 6, top panel). The best indicator of decreased helicity is the change in the $\pi-\pi^*$ component located below 200 nm. Upon cooling of the sample, the original spectra were recovered indicating that the process was reversible. Similar trends were observed for the other helical transmembrane peptides in SDS micelles (data not shown). The β-like CD pattern of M6-31 varied very little on raising the temperature to 85 °C (Figure 6, bottom panel). The negative ellipticity at 215 nm is almost identical at all temperatures. However, the ellipticity near 200 nm shifts and decreases as the temperature is raised. Again, the CD spectra were reversible on cooling (data not shown). Similar results were found for M3-35 (data not shown). These observations indicated the high thermostability of the conformations assumed by all of the transmembrane peptides in a variety of membrane mimetic solvents.

In a previous investigation, we studied the influence of a mutation of Pro258 to Leu on the structure of M6-18 because this mutation in native Ste2p results in a constitutively active receptor possibly due to a conformational change that activates the receptor without the necessity of ligand binding (*40*). However, all attempts to investigate this same mutation in M6-31 failed because we could not purify the peptide due

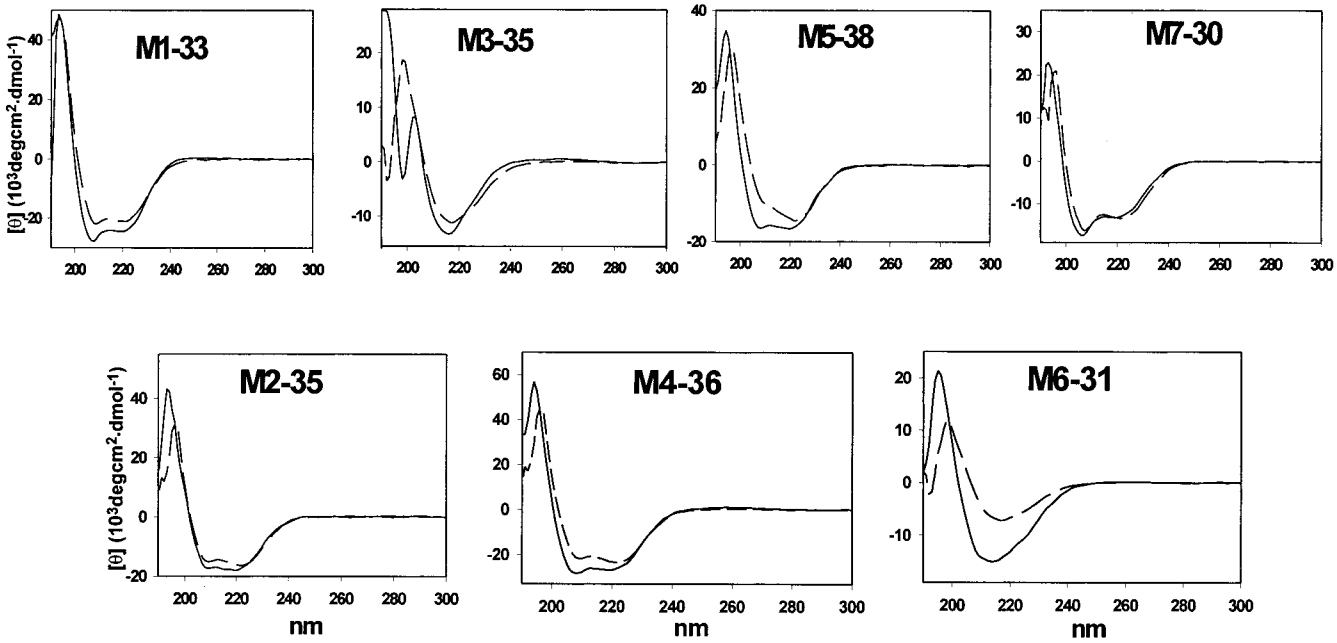

FIGURE 4: CD spectra of synthetic membrane peptides in SDS micelles and DMPC vesicles. In each panel, the solid line represents the indicated peptide dissolved in 0.5% SDS buffer and the dashed line represents the peptide prepared in the presence of 3.6 mM DMPC. The final peptide concentrations ranged from 10 to 30 μM.

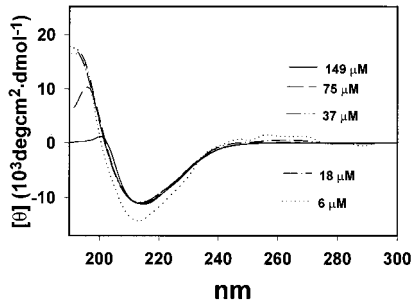

FIGURE 5: CD spectra of M6-31 at different concentrations in SDS micelles.

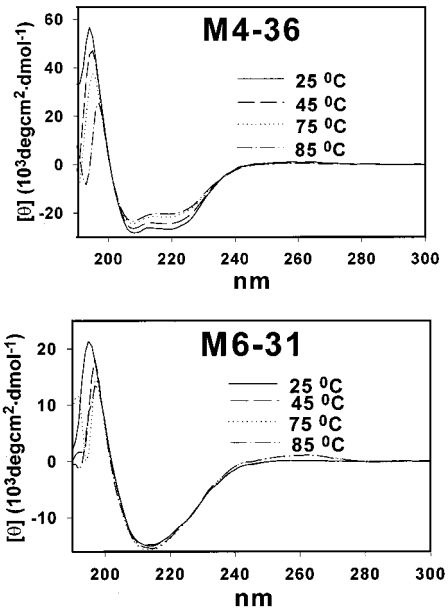

FIGURE 6: Thermal stability of 2° structures of synthetic membrane peptides in SDS micelles. Top panel: a representative α-helical peptide, M4-36; concentration 12 μM. Bottom panel: a representative β-like peptide, M6-31; concentration 36 μM.

to its extremely poor solubility (*20*). To circumvent this problem, we added Lys residues to both the extracellular and cytoplasmic sides of the sixth transmembrane domain (Table 1). The CD patterns of M6-35L and M6-35P in SDS and DMPC environments differ significantly from those of M6-31 (Figure 7). Both of the peptides with the lysine extensions show significantly more helicity. As judged by the magnitude of the ellipticity at 222 nm and the splitting of the $\pi-\pi^*$ transition, M6-35P is intermediate in helicity as compared to M6-35L and M6-31. Quantitative calculations show that the helicity of M6-35L varies from 84% to 69% as the water content in trifluoroethanol is changed from 0% to 75%. M6-35P exhibits helicities from 68% to 48% in the same solvent mixtures. The leucine containing peptide is 51% and 43% helical in SDS micelles and DMPC bilayers, respectively, whereas M6-35P is 40% and 33% helical under these conditions (Table 3).

IR Analysis of the Sixth Transmembrane Domain

The correlation between the frequency of amide I vibrational mode (primarily a carbonyl stretching mode) and the nature of the secondary structure has been well established in the literature (*41*). Frequencies in the regions of 1650−1660 cm^{-1} correspond to α-helical segments while modes resonating in the regions of 1630−1640 cm^{-1} and 1670−1685 cm^{-1} correspond to β-sheet elements. Further assessment of the M6 peptides was conducted using infrared spectroscopy. Attempts to prepare peptide DMPC bilayers on CaF_2 crystals were unsuccessful. However, stable bilayers on crystal surfaces were prepared using DMPC/DMPG (4:1) mixtures. Under these conditions, M6-35L and M6-35P showed significantly different IR patterns in both the amide I and amide II regions. In particular, M6-35L showed a peak at 1656 cm^{-1} with a shoulder at about 1635 cm^{-1}, whereas M6-35P showed a more complex series of bands in the amide I region with absorbance at 1685 cm^{-1}, 1653 cm^{-1} and a

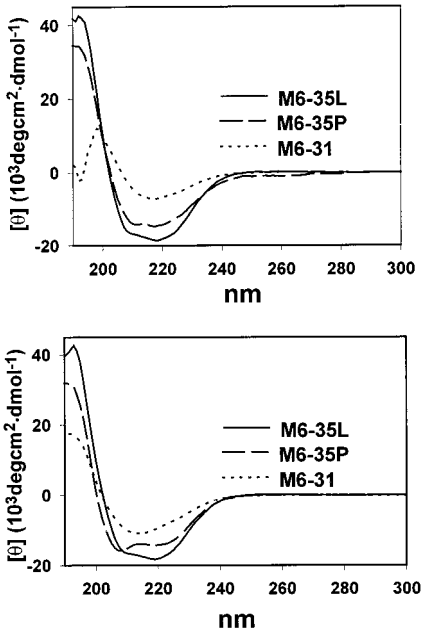

FIGURE 7: CD spectra of M6 fragments: top, DMPC vesicles; bottom, SDS micelles. In each panel, the solid line represents M6-35L, the dashed line represents M6-35P, and the dotted line represents M6-31. The final peptide concentrations ranged from 10 to 40 μM.

Table 3: Calculated Helicities (%) of Various Sixth Transmembrane Domain Peptides[a]

	TFE/water				0.5%	3.6 mM
peptide	100%	75%	50%	25%	SDS	DMPC
M6-35L	84	77	75	69	51	43
M6-35P	68	63	57	48	40	33
M6-31	57	43	44	27	*b*	*b*

[a] Calculated using $[\theta]_{222}$ values (see Experimental Procedures). [b] Not calculated due to low α-helicity.

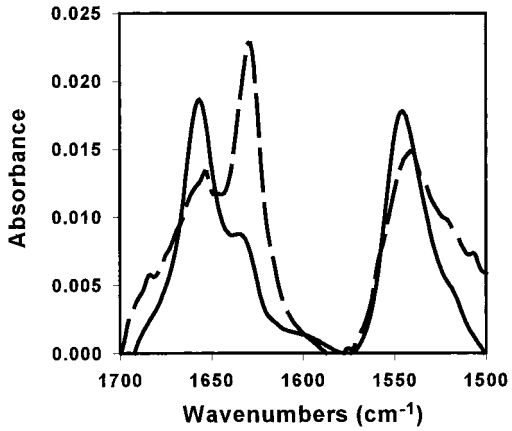

FIGURE 8: FTIR of amide I and amide II regions of the sixth transmembrane domain peptides. The solid line is for M6-35L in DMPC/DMPG (4:1) bilayers. The dashed line is for M6-35P under identical conditions. The calculated molar ratio of peptides to lipid was 1:108.

major band centered at 1629 cm^{-1} (Figure 8). The amide II absorbencies had maxima at 1546 and 1541 cm^{-1} for M6-35L and M6-35P, respectively. These results show that under the conditions used both peptides have mixed conformations with M6-35L predominantly helical and M6-35P predominantly a β-structure. Under identical conditions, the IR spectrum of M6-31 was consistent with a β-structure (data not shown).

Fluorescence Spectroscopy on Tryptophan-Containing Transmembrane Peptides

The analysis of the environment of the transmembrane peptides was further assessed using fluorescence spectroscopy. Both M1-33 and M7-30 contain Trp residues that are predicted to be inside the lipid interior of the membrane (Figure 1). Trp fluorescence of M1-33 in MeOH solution and in the presence of DMPC vesicles showed emission maxima of 350 and 344 nm, respectively (Figure 9A). Thus, the environment of the Trp residue of M1-33 in the DMPC vesicle suspension is slightly less polar than methanol. Fluorescence-quenching experiments using KI as the quencher gave linear plots of F_0/F vs [I$^-$] (Figure 9B). The derived Stern−Volmer constant (K_{sv}) was 2.11 M^{-1}. By comparison, K_{sv} = 5.88 M^{-1} for the same peptide in methanol. These results are similar to those observed for M7-30 (data not shown) and suggest that the lipids effectively shield the Trp from collision with iodide.

Tricine−SDS-PAGE Studies on Transmembrane Peptides

SDS polyacryalamide gel electrophoresis (SDS-PAGE) was run to assess the molecular size of the peptides in the presence of detergent micelles. The seven transmembrane peptides ran as bands of various breadth when the peptides were electrophoresed on 27.7% gels in a Tricine−SDS buffer (Figure 10). Attempts were made to apply similar amounts of peptide to the gel. Nevertheless, bands of very different size resulted, and the staining efficiencies varied from peptide to peptide (compare gel B, lane h with gel A, M4). In fact, several of the peptides did not stain at all using Coomassie Blue (data not shown). Nevertheless, except for M6-31, the monomeric form of each peptide is visible near the bottom of their corresponding lanes (Figure 10A). M6-31 mainly self-associates (a faint band is seen near the monomer molecular weight) and forms a higher molecular species containing 7−8 molecules. Lowering concentration of M6-31 to 6 μM did not significantly affect its multimeric state (Figure 10B). In the case of M3, a significant band was observed at the stacking gel along with a broad band with a slight split moving as a monomer (Figure 10A, M3).

Comparison of M6-31, M6-35P, and M6-35L using SDS-PAGE revealed that the leucine mutant peptide moved predominantly as a monomer, whereas at similar concentrations M6-35P was a mixture of low and high molecular weight species. At very high concentrations, both M6-31 and M6-35P showed a number of different high-molecula-weight forms. However, as stated above, even at very low concentrations M6-31 would not form a monomer in the gel (Figure 10B, lanes f and g).

DISCUSSION

Transmembrane domains are predicted to assume an α-helical secondary structure because this is the most stable structure in the hydrophobic interior of the lipid bilayer (*42*). Direct biophysical evidence for this secondary structure in a GPCRs comes from studies with rhodopsin, a photoreceptor (*43*, *44*). The low-resolution structure deduced for the transmembrane core of rhodopsin reveals seven helical

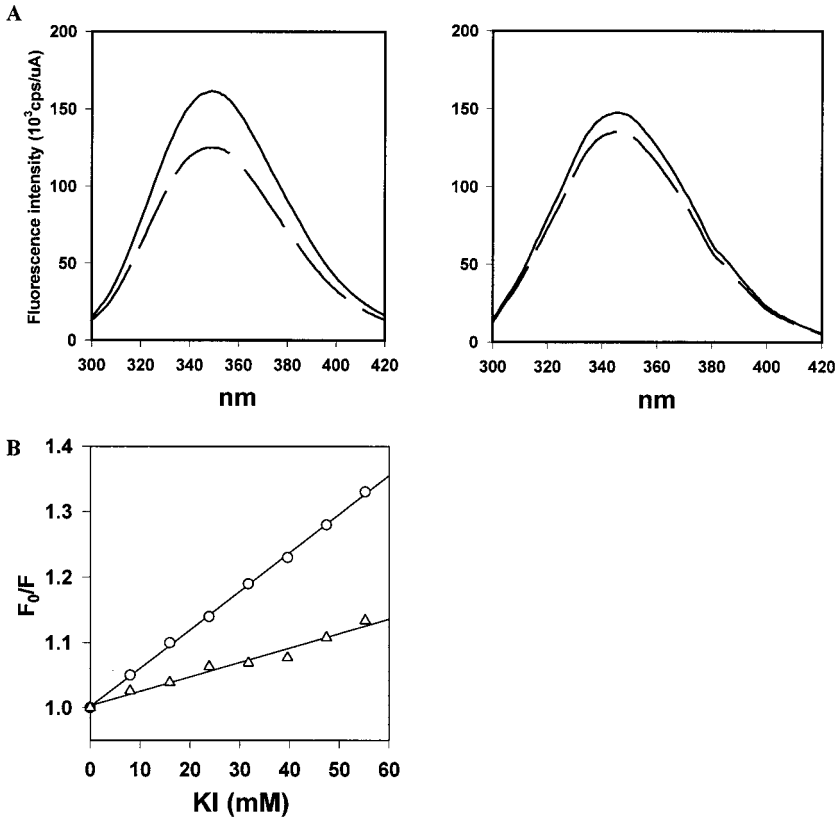

FIGURE 9: (A) Fluorescence emission of M1-33 in the presence of KCl (50 mM, solid line) or KI (50 mM, dashed line): left, in MeOH; right, in DMPC vesicles. Both peptide concentrations are 2.5 μM. (B) Stern−Volmer Plot for M1-33 in DMPC vesicles (△) and MeOH (○).

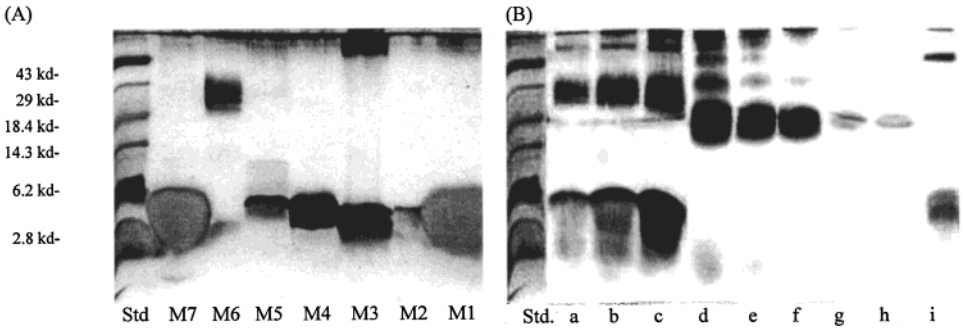

FIGURE 10: Tricine SDS-PAGE of synthetic membrane peptides. A total of 20 μL of each peptide sample was loaded to its respective lane. (A) M1−M7. Peptide concentrations: [M1] = 10 μM, [M2] = 5.3 μM, [M3] = 11.1 μM, [M4] = 6.3 μM, [M5] = 8 μM, [M6] = 18.0 μM, [M7] = 19 μM. (B) M6-35P (lanes a−c), M6-31 (lanes d−h), and M6-35L (lane i). Peptide concentration: a, 18 μM; b, 36 μM; c, 72 μM; d, 75 μM; e, 37 μM; f, 18 μM, g, 9 μM; h, 6 μM; i, 14 μM.

regions with different tilts and with discontinuities that are interpreted as kinks in the helical structures. This structure has served as a basis for comparison with other conformational data on GPCRs. Due to the lack of good crystals for any other GPCRs and the high molecular weight of these membrane bound proteins, indirect approaches have been used for their structural analysis. Specifically, rather than study the entire protein, individual transmembrane domains are examined to learn about the intact protein.

Previous investigations of synthetic peptide model compounds to study the biophysical properties of GPCRs have been very limited. To our knowledge in only one case have the synthesis and characterization of all the transmembrane domains of a heptahelical protein, bacteriorhodopsin, been reported (*21*). This photoreceptor is not coupled to G proteins. In another elegant study, 6 of the putative 12 transmembrane peptides of the cystic fibrosis chloride transporter were synthesized and characterized (*45*). Before comparison of our biophysical results with those of these studies, it is instructive to discuss some synthetic aspects.

As indicated in the Results , the synthesis of transmembrane peptides is challenging due to their poor solubility and tendency to aggregate. The average hydrophobicities (*29*) of the portions of the synthetic peptides that are in the interior of the membrane were calculated to vary from 1.46 to 2.36 (Table 1). Interestingly, the two most difficult domains to synthesize, M3 and M4, had relatively low hydrophobicities. Thus, it is clear that the average hydrophobicity does not account for the difficulties encountered during synthesis of M3 and M4 and that specific sequence dependent effects must be important. The addition of several lysine residues (see below for further discussion) at the carboxyl and amino

ends of M3 and M4 resulted in more soluble peptides, which could be purified using the strategies discussed earlier.

Biophysical experiments were carried out on the putative seven synthetic transmembrane fragments of Ste2p (M1−M7) and two variants of M6 (M6-35P and M6-35L). All peptides studied in this investigation have a similar chain length of 30−38 amino acid residues. On the basis of CD results in TFE−water mixtures, the seven transmembrane domains have a high proclivity to assume α-helical structures (Figure 3, Table 2). Indeed, in 100% TFE the percent helicity ranges from 57% to 86%. However, titration with water begins to reveal the conformational differences in the various regions of this GPCRs. M6-31 is only 27% helical in 25% TFE/75% water and exhibits a CD pattern which is not characteristic of an α-helix, whereas M4-36 is still 75% helical in the identical solvent.

In contrast to the helicity found for all peptides in aqueous TFE, the membrane peptides exhibited significant structural diversity in SDS and DMPC environments. Several peptides (e.g., M4-36) retained high helicity in both micelles and bilayers. Others such as M3-35 and M6-31 formed β-structures. Fluorescence studies in DMPC on both M1-33 and M7-30, the two transmembrane domains that contained Trp residues, showed that the aromatic residue is in the lipid environment and protected from quenching by a hydrophilic iodide anion. Thus, it is reasonable to conclude that these peptides do insert into the lipid bilayers. We observed that the method of sample preparation was very important in determining the conformational state of the peptides in SDS and DMPC. It was critical to allow the peptide to reach equilibrium with the lipid environment of either the micelle or the bilayer. Direct attempts to sonicate several of the peptides in the presence of either SDS or DMPC resulted in either very poor spectra (no incorporation) or β-like CD patterns. In contrast, when the peptide was equilibrated by dialysis with these membrane mimetic environments, helical structures sometimes resulted. The conclusions with CD have been verified using ATR−FTIR analysis (Ding, personal communication). Similar observations concerning sample preparation were reported for the bacteriorhodopsin transmembrane domains (*21*). Given the care taken to prepare all samples under identical conditions, the conformational tendencies of M3-35 and M6-31 are especially significant. The β-structure formed by M6-31 is very stable. It existed over a 30-fold range of concentration (Figure 5) and was stable up to 85 °C (Figure 6, bottom). As the helix formed by peptides such as M4-36 was also stable to relatively high temperatures (Figure 6 top) and as the CD spectra were reversible on heating, it is reasonable to conclude that the CD patterns represent the thermodynamically stable forms of these peptides in the lipidlike media.

Gel electrophoresis of the transmembrane domains gave support to the conclusions from CD analysis in SDS micelles. At similar concentrations, helical peptides M1-33, M2-35, M4-36, M5-38, and M7-30 all ran as monomers (Figure 10). In contrast, the two peptides, which gave β-like CD patterns, ran as either an oligomeric species (M6-31) or as a monomer plus a higher MW band (M3-35). The oligomer of M6-31 (approximately seven or eight peptide chains) exists over at least a 10-fold concentration range. One can conclude that M3 and M6 have a much greater tendency to self-associate than the other transmembrane peptides of Ste2p.

The observation of β-sheet structures for M3 and M6 in detergent and lipids is to some extent unexpected. A β-structure was also reported for a transmembrane fragment (domain G) from bacteriorhodopsin (*21*). These observations support the conclusion that the conformation of the transmembrane domains of intact receptors is not determined simply by the secondary structural propensity of the isolated fragments but is further influenced by long-range interactions within the protein. This conclusion suggests that the two-step model (*12*) would not account for all features of the folding of Ste2p.

Recently, a high-resolution crystal structure of rhodopsin revealed intramolecular interactions between various transmembrane regions (*11*). These regions are stabilized by a number of interhelical hydrogen bonds and hydrophobic interactions, most of which are mediated by highly conserved residues. Interestingly, Arg^{135} in helix H-III interacts with Glu^{247} and Thr^{251} in helix H-VI. It is tempting to conclude that such interactions are a general feature in all GPCRs, and domains III and VI in Ste2p are similarly in contact. Indeed, several studies have demonstrated that helix−helix interactions are necessary for receptor activation (*46*−*48*). This perspective would allow us to propose that lack of domain−domain interactions for the isolated M3 and M6 fragments could account for the failure of these peptides to form stable helices in micelles and lipids. We note that Ste2p lacks the conserved Glu^{134}-Arg^{135}-Tyr^{136} tripeptide of helix III of rhodopsin and does not have corresponding residues in helix VI. It also belongs to a distinct subfamily of GPCRs that only includes fungal receptors (*49*). Therefore, definitive information on the interaction between M3 and M6 in Ste2p will require high-resolution studies on the intact receptor.

As an α-helix → β-sheet transition was observed for M6-31 when the solvent was changed from TFE−water to either DMPC vesicles or SDS micelles, this receptor domain also manifests significant conformational flexibility. The tendency of domain 6 to be conformationally flexible may be biologically significant. Greater than 90% of all GPCRs contain a proline residue at similar positions in transmembrane domain 6. Mutation of these proline residues often has biological consequences. For example, Ste2p mutation of Pro258 to Leu resulted in constitutive activity with 45% of the saturable wild-type signaling in the absence of pheromone (*40*, *50)*. The current model of signal transduction by G protein-coupled receptors involves the isomerization of the receptor from an inactive to an active form. Using mutational analysis, the sixth transmembrane domain and the third cytoplasmic loop were implicated in receptor activation (*51*−*53*) and polar residues in transmembrane domain 6 of Ste2p were suggested to interact with other domains of the receptor (*54*). Previously we reported that an 18-residue homologue, M6-18L (252−269, C252A, P258L) corresponding to the constitutively active receptor Ste2p−P258L, was a highly α-helical structure in SDS micelles but was a β-structure in HFA−water (*20*). However, the synthesis of the 31-residue homologue M6-31L (239−269, C252A, P258L) failed due to extreme aggregation. In this study, CD analyses indicated that a soluble variant of M6 (M6-35L, Table 1) is highly helical in the three membrane mimetic environments examined (Table 3 and Figure 7). The wild-type homologue M6-35P is decidedly less helical. Moreover, FTIR analysis indicates that in DMPC/DMPG (4:1), M6-35L is predomi-

nantly α-helical whereas M6-35P is predominantly a β-sheet structure (Figure 8). Interestingly, in SDS-PAGE studies, M6-35P forms a mixture of monomer and aggregated forms whereas M6-35L forms mostly monomer forms (Figure 10B). Thus, if one hypothesizes that the activated receptor involves stabilizing a state wherein the sixth transmembrane domain forms a helical structure, then both the CD, IR, and gel studies suggest that the Pro258Leu mutation would favor this helical structure. Although Pro has often been considered to be a potent α-helix breaker, studies in membrane mimetic solvents concluded its conformational tendencies are highly environment sensitive (*55*). Moreover, we have recently shown that after extensive mutagenesis only a limited spectrum of mutations in Ste2p lead to a constitutively activated receptor and that a number of these mutations are in the sixth transmembrane domain (*50*). Thus, it is not unreasonable to suggest that the Pro258 serves as a conformational switch for Ste2p. However, this hypothesis requires that the conformational tendencies of the fragments represent the physiological situation in intact Ste2p. Obviously, only detailed structural studies on the active and inactive receptor can test this hypothesis.

The idea of oligomerization of GPCRs is gaining credence from a variety of investigations (for review, see ref *56*) including one report where transmembrane peptides inhibited dimerization of β-adrenergic receptor (*57*). M6 was found to self-aggregate using SDS-PAGE analysis, and M3 also forms high-molecular-weight species on SDS gels (Figure 9A). In preliminary studies we found that M6 also tends to interact with other domains as judged by gel electrophoresis analysis (Xie and Arevalo, unpublished results). Since a recent study demonstrated that Ste2p is oligomeric in intact cells and membranes of *S. cerevisiae* (*58*), our results suggest that Ste2p might form dimers through a direct interaction of specific transmembrane domains having a tendency to aggregate due to their biophysical properties.

An aspect of this study that requires consideration is the influence of the additional lysine residues on the structure of the central core in the transmembrane peptides. It was our belief that placing several lysines on both sides of the domain would prevent aggregation due to hydrophobic stacking of the central core. Other scientists working with membrane peptides have used lysine residues to solubilize these molecules (*30*, *31*), and this approach was used many years ago to solubilize poly-L-alanine (*59*). Our data support the conclusion that the hydrophilic chain ends do not significantly affect the helix formation by residues in the center of the peptide. Study of the series of peptides representing different lengths of M2 showed that M2-25 was the most helical, whereas M2-20 and M2-35 had similar percent helicities. Assuming the model in Figure 1, 76% (19/25) of the residues of M2-25 should be helical. For M2-35, 66% (23/35) should be helical. This calculation is in excellent agreement with the CD results in 50% aqueous TFE. One would conclude then that the extramembranous portions of the model peptides assume random structures. A comparison of the CD profiles and the SDS gels and the IR spectra of M6-31 and M6-35P indicates that the peptide without the lysine residues does have a greater tendency to aggregate. Nevertheless, the comparison of the same data for M6-35P and the mutant peptide M6-35L shows that the lysine extensions do not conceal the different conformational tendencies of these molecules. Finally, both M3-35 and M4-36 contain similar extensions on the carboxyl and amine terminus, yet one of these peptides is highly helical in SDS and DMPC environments whereas the other is a β-aggregate. We conclude that useful information on the inherent conformational tendencies of a transmembrane domain can be obtained using oligolysine substitutions in the hydrophilic loops of the receptor; however, one should be careful in the interpretation of the results. Conjugation with poly(ethylene glycol) has also been suggested as an approach to enhance the solubility of transmembrane domains in aqueous media (*60*). The generality of this solubilizing group needs to be systematically explored with different domains.

As stated above, the seven transmembrane peptides of bacteriorhodopsin were previously subjected to detailed analysis using CD, FTIR, and proteolysis experiments (*21*). The authors found that the first five transmembrane domains formed stable α-helical structures in detergent and lipids, whereas the sixth domain did not have a stable structure and the seventh domain formed a hyperstable β-sheet structure. More recently, five of the first six transmembrane peptides of the CFTR receptor were found to be helical whereas the sixth domain underwent a shift from an α-helix to a β-structure in 20% methanol (*45*). Our results on Ste2p show that most of the domains of this receptor were helical but that two of the domains, M3 and M6, could form β-structures. Finally, a recent solution NMR study on the sixth transmembrane peptide of rhodopsin in DMSO-d_6 concluded that this domain was helical throughout most of its length and that the Pro residue induced only a small distortion in the helix (*25*). Our NMR studies on an 18-residue fragment of the sixth transmembrane of Ste2p in TFE−water indicated that the helix formed by this peptide is kinked (*20*) and that this domain may be conformationally diverse (vida supra). The high-resolution structure of rhodopsin showed that there was a significant bend at Pro^{267} of the sixth transmembrane helix (*11*). It seems clear that transmembrane peptides of integral membrane proteins will have individual biophysical tendencies and that they will not all simply behave as rigid helical rods.

In conclusion, the results presented herein represent the first complete analysis of all membrane segments of one GPCR. The analysis shows that despite the helical proclivity of the transmembrane regions of Ste2p each domain is unique in its biophysical properties. In particular, two domains M3 and M6 showed a higher tendency than the other peptides to aggregate and form β-structures and domain 6 may be a conformationally flexible region of the receptor. These findings lead us to suggest that domain 6 may be involved in a conformational transition during receptor activation and that this domain and domain 3 may be involved in domain−domain interactions which result in isomerization and/or receptor oligomerization.

REFERENCES

1. Dohlman, H. G., Thorner, J., Caron, M. G., and Lefkowitz, R. J. (1991) *Annu. Rev. Biochem. 60*, 653−688.
2. Wess, J. (1997) *FASEB J. 5*, 346−353.
3. Gether, U. (2000) *Endocrine Rev. 21*, 90−113.
4. Josefson, L.-G. (1999) *Gene 239*, 333−340.
5. Flower, D. R. (1999) *Biochim. Biophys. Acta 1422*, 207−234.
6. Lomize, A. L., Pogozheva, I. D., and Mosberg, H. I. (1999) *J. Comput.-Aided Mol. Des. 13*, 325−353.

7. Pebay-Peyroula, E., Rummel, G., Rosenbusch, J. P., and Landau, E. M. (1997) *Science (Washington, D.C.) 277*, 1676−1681.
8. Grigorieff, N., Ceska, T. A., Downing, K. H., Baldwin, J. M., and Henderson, R. (1996) *J. Mol. Biol. 259*, 393−421.
9. Kimura, Y., Vassylyev, D. G., Miyazawa, A., Kidera, A., Matsushima, M., Mitsuoka, K., Murata, K., Hirai, T., and Fujiyoshi, Y. (1997) *Nature 389*, 206−211.
10. Baldwin, J. M. (1993) *EMBO J. 12*, 1693−1703.
11. Palczewski, K., Kumasaka, T., Hori, T., Behnke, C. A., Motoshima, H., Fox, B. A., Trong, I. L., Teller, D. C., Okada, T., Stenkamp, R., Yamamoto, M., and Miyano, M. (2000) *Science 289*, 739−745.
12. Popot, J. L., and Engelman, D. M. (1990) *Biochemistry 29*, 4031−4037.
13. Huang, K. S., Bayley, H., Liao, M. J., London, E., and Khorana, H. G. (1981) *J. Biol. Chem. 256*, 3802−3809.
14. London, E., and Khorana, H. G. (1982) *J. Biol. Chem. 257*, 7003−7011.
15. Kahn, T. W., and Engelman, D. M. (1992) *Biochemistry 31*, 6144−6151.
16. Ozawa, S., Hayashi, R., Masuda, A., Iio, T., and Takahashi, S. (1997) *Biochim. Biophys. Acta 1323*, 145−153.
17. Marti T. (1998) *J. Biol. Chem 273*, 9312−9322.
18. Ridge, K. D, Lee, S. S, and Yao, L. L. (1995) *Proc. Natl. Acad. Sci. U.S.A. 92*, 3204−3208.
19. Reddy, A. P., Tallon, M. A., Becker, J. M., and Naider, F. (1994) *Biopolymers 34*, 679−689.
20. Arshava, B., Liu, S. F., Jiang, H., Breslav, M., Becker, J. F., and Naider, F. (1998) *Biopolymers 46*, 343−357.
21. Hunt, J. F., Earnest, T. N., Boushe, O., Kalghatgi, K., Reilly, K., Horvath, C., Rothschild, K. J., and Engelman, D. M. (1997) *Biochemistry 36*, 15156−15176.
22. Dorey, M., Hargrave, P. A., McDowell, J. H., Arendt, A., Vogt, T., Bhawsar, N., Albert, A. D., and Yeagle, P. L. (1999) *Biochim. Biophys. Acta 1416*, 217−224.
23. Yeagle, P. L., Alderfer, J. L., Salloum, A. C., Ali, L., and Albert, A. D. (1997) *Biochemistry 36*, 3864−3869.
24. Yeagle, P. L., Alderfer, J. L., and Albert, A. D. (1995) *Nat. Struct. Biol. 2*, 832−834.
25. Chopra, A., Yeagle, P. L., Alderfer, J. A., and Albert, A. D. (2000) *Biochim. Biophys. Acta 1463*, 1−5.
26. Martin, N. P., Leavitt, L. M., Sommers, C. M., and Dumont, M. E. (1999) *Biochemistry 38*, 682−695.
27. Cartwright, C. P., and Tipper, D. J. (1991) *Mol. Cell. Biol. 11*, 2620−2628.
28. Harley, C. A, and Tipper, D. J. (1996) *J. Biol. Chem. 271*, 24625−24633.
29. Kyte, J., and Doolittle, R. F. (1982) *J. Mol. Biol. 157*, 105−132.
30. Bianchi, E., Ingenito, R., Simon, R. J., and Pessi, A. (1999) *J. Am. Chem. Soc. 121*, 7698−7699.
31. Chen, C. C., Kao, J., and Marshall G. R. (1999) The 16th American Peptide Symposium, Poster 681, Minneapolis, MN.
32. Schagger, H., and von Jagow, G. (1987) *Anal. Biochem. 166*, 368−379.
33. Greenfield, N., and Fasman, G. D. (1969) *Biochemistry 8*, 4108−4116.
34. Wu, C. S. C., Ikeda, K., and Yang, J. T. (1981) *Biochemistry 20*, 566−570.
35. Chen, Y. H., Yang, J. T., and Chau, K. H. (1974) *Biochemistry 13*, 3350−3359.
36. Kent, S. B. (1988) *Annu. Rev. Biochem. 57*, 957−989.
37. Grebow, P. E., and Hooker, T. M., Jr. (1975) *Biopolymers 14*, 871−881.
38. Ziegler, S. M., and Bush, C. A. (1971) *Biochemistry 10*, 1330−1335.
39. Johnson, W. C. (1988) *Annu. Rev. Biophys. Biophys. Chem. 17*, 145−166.
40. Konopka, J. B., Margarit, S. M., and Dube, P. (1996) *Proc. Natl. Acad. Sci. U.S.A. 93*, 6764−6769.
41. Braiman, M. S., and Rothschild, K. J. (1988) *Annu. Rev. Biophys. Biophys. Chem. 17*, 541−570.
42. Engelman, D. M., Steitz, T. A., and Goldman, A. (1986) *Annu. Rev. Biophys. Biophys. Chem. 15*, 321−353.
43. Schertler, G. F. X., Villa, C., and Henderson, R. (1993) *Nature (London) 362*, 770−772.
44. Urger, V. M., and Schertler, G. F. X. (1995) *Biophys. J. 68*, 1776−1786.
45. Wigley, W., Vijayakumar, S., Jones, J. D., Slaughter, C., and Thomas, P. J. (1998) *Biochemistry 37*, 844−853.
46. Dube, P., and Konopka, J. B. (1998) *Mol. Cell. Biol. 18*, 7205−15.
47. Tarasava, N. I., Rice, W. G., and Michejda, C. J. (1999) *J. Biol. Chem. 274*, 34911−34915.
48. Feng, Y. H., and Karnik, S. S. (1999) *J. Biol. Chem. 274*, 34546−34552.
49. Horn, F., Weare, J., Beukers, M. W., Horsch, S., Bairoch, A., Chen, W., Envardsen, O., Campagne, F., and Vriend, G. (1998) *Nucleic Acids Res. 26*, 277−281.
50. Sommers, C. M., Martin, N. P., Akal-Strader, A., Becker, J. M., Naider, F., and Dumont, M. E. (2000) *Biochemistry 39*, 6898−6909.
51. Clark, C. D., Palzkill, T., and Botstein, D. (1994) *J. Biol. Chem. 269*, 8831−8841.
52. Stefan, C. J., and Blumer, K. J. (1994) *Mol. Cell. Biol. 14*, 3339−3349.
53. Weiner, J. L., Guttierez-Steil, C., and Blumer, K. J. 1993. *J. Biol. Chem. 268*, 8070−8077.
54. Dube, P., and Konopka, J. B. (1998) *Mol. Cell. Biol. 18*, 7205−7215.
55. Li, S. C., Goto, N. K., Williams, K. A., and Deber, C. M. (1996) *Proc. Natl. Acad. Sci. U.S.A. 93*, 6676−6681.
56. Hebert, T. E., and Bovier, M. (1998) *Biochem. Cell Biol. 76*, 1−11.
57. Hebert, T. E., Moffett, S., Morello, J. P., Loisel, T. P., Bichet, D. G., Barret, C., and Bouvier, M. (1996) *J. Biol. Chem. 271*, 16384−16392.
58. Overton, M. C., and Blumer, K. J. (2000) *Curr. Biol. 10*, 341−344.
59. Ingwall, R. T, Scheraga H. A, Lotan N., Berger A., and Katchalski E. (1968) *Biopolymers 6*, 331−68.
60. Pomroy, N. C., and Deber, C. M. (1999) *Anal. Biochem. 275*, 224−230.

BI001432P